

# A Whole body Physiologically based Pharmacokinetic Model for Antibody drug conjugates – model development and validation in rat

Linzhong Li<sup>1</sup>, Shang-Chiung Chen<sup>2</sup>, Felix Stader<sup>1</sup>, Rachel Rose<sup>1</sup>, Indranil Rao<sup>1</sup>, Iain Gardner<sup>1</sup>, Masoud Jamei<sup>1</sup>, Ben-Quan Shen<sup>2</sup>, Victor Yip<sup>2</sup>, Yuan Chen<sup>2</sup>, Jin Yan Jin<sup>2</sup>, Chunze Li<sup>2</sup>

(1) Simcyp (A Certara Company), Blades Enterprise Centre, Sheffield, UK (2) Genentech, Inc, 1 DNA Way, South San Francisco, CA 94080, USA.

**Objectives:** To develop and qualify a whole body physiologically-based pharmacokinetic (PBPK) model for simulating Antibody Drug Conjugate (ADCs) disposition in rat tissues.

**Methods:** The whole body PBPK approach adapted here combines features of a previously published minimal PBPK model for mAbs [1] and a compartmental model for ADCs [2], see Figure 1. The base model incorporates tissue-specific data related to IgG transport via both convection/diffusion and an FcRn-mediated pathway, including (1) tissue-dependent FcRn expression (derived from data in transgenic mice [3]), (2) an estimate of tissue endosomal volume, (3) tissue lymphatic flows, (4) predicted vascular reflection coefficients [4], and (5) tissue-dependent recycling rates [5]. This base model is applied to all ADC DAR (Drug Antibody Ratio) species, which are subject to deconjugation, catabolism, target-mediated elimination, and other additional clearance processes, resulting in release of the payload. The releasing fluxes of payload are directly fed into a full PBPK model for the small molecule drug and is thus treated as a metabolite of the ADC. Target binding models to account for target mediated disposition (TMD) can be applied to plasma and interstitial space of any tissue in any combination. The ADC model parameterised with DAR-dependent information allows simulation studies on various factors which influence ADC disposition to be conducted.

Model verification was performed using *in vivo* rat data to qualify the model in four steps: (1) matching rat IgG plasma and tissue profiles in rat to fix model parameters for IgG kinetics, (2) matching the plasma profile of the naked monoclonal antibody (mAb) for a vc-MMAE ADC to fix the base model parameters for the ADC, (3) matching plasma profiles for the vc-MMAE ADC by incorporating a DAR-dependent plasma clearance, and (4) predicting tissue profiles of the vc-MMAE ADC.

In addition, plasma incubation studies with the ADC were conducted (Figure 3 (B)) and used to derive *in vitro* deconjugation rates. This set of *in vitro* deconjugation rates is directly applied to plasma in simulations; deconjugation rate constants in tissue interstitial spaces are scaled down by taking 20% of these *in vitro* deconjugation rates. To check mass balance, three quantities are calculated, (1) percentage of eliminated antibody relative to total injected antibody, (2) percentage of eliminated MMAE relative to total injected MMAE, and (3) ratio of eliminated MMAE to released MMAE.

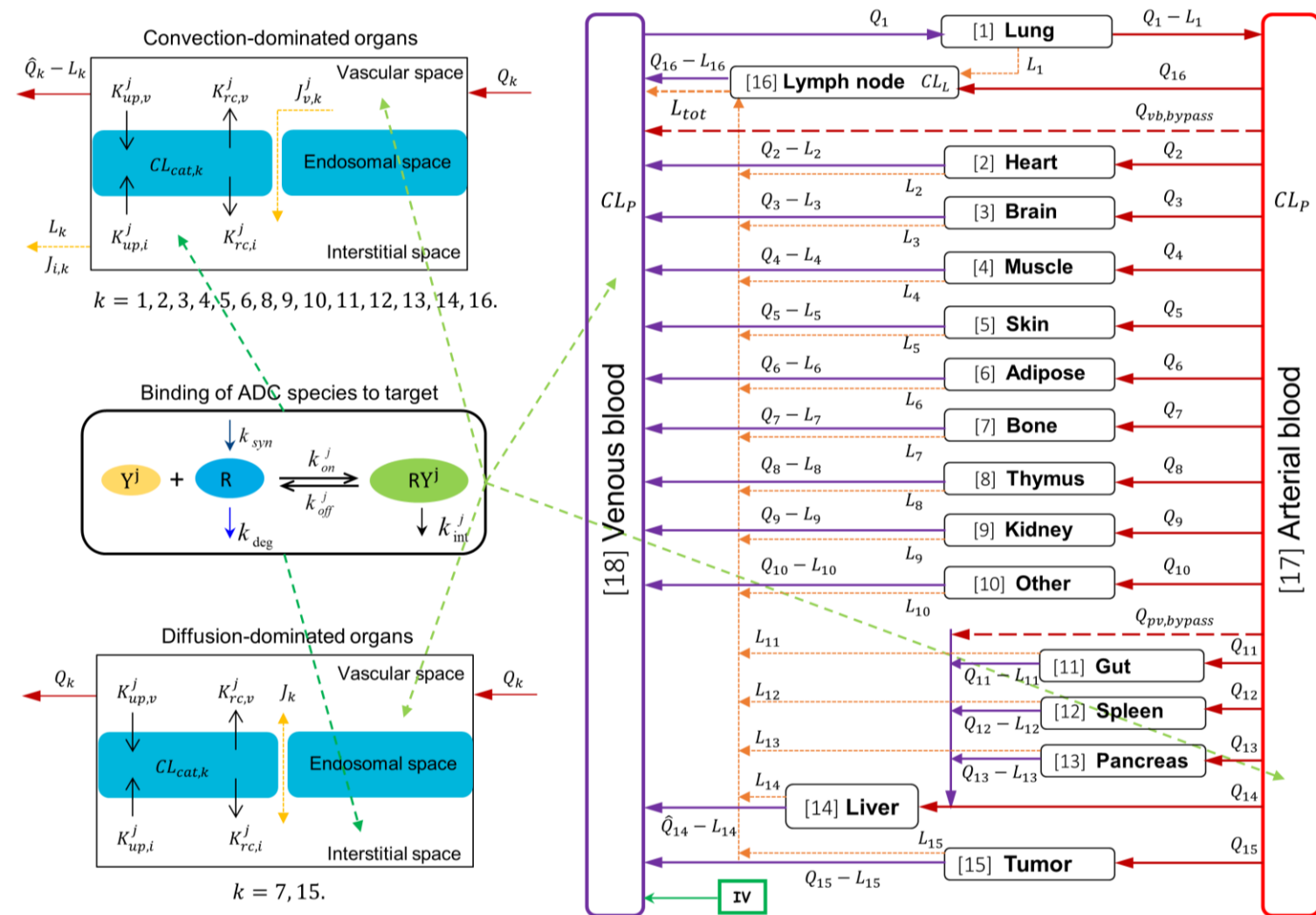


**Figure 1** A generic model structure for both mAb and ADCs. Subscript *k* represents tissue/organ and superscript *j* denotes ADC DAR species. All tissues/organs are modelled as being convection-dominated in the transport of antibody except bone and (solid) tumor, which are treated as being diffusion-dominated. Competitive binding between endogenous IgG and exogenous IgG (mAbs or ADC species) for FcRn are considered in all tissues/organs where FcRn is expressed.

**Results: Rat IgG kinetics:** The base model adequately describes IgG kinetics in rat, see Figure 2. The mean IgG profile of a group of male Sprague-Dawley rats [7] is matched very well with a associated half-life of 7.8 days. The model parameters for the binding affinity of rat IgG to rat FcRn, fluid-phase uptake rate constant, and total catabolic clearance are 0.329 ( $\mu\text{M}$ ) [8], 0.104 (1/h), and 0.172 (mL/h), respectively. Turning off FcRn pathway in the model to mimic a FcRn-deficient rat generates a plasma profile with 8 fold increase in clearance. IVIG simulations with very high doses were done to demonstrate the competitive effect in the FcRn-mediated pathway.

**Naked Antibody profile:** The antibody is a humanized IgG1. It was found that once the difference of the binding affinity between human IgG to rat FcRn and rat IgG to rat FcRn is corrected, the observed profile for the naked Ab can be matched well by calibrating the fluid-phase uptake rate alone, see Figure 3 (A).

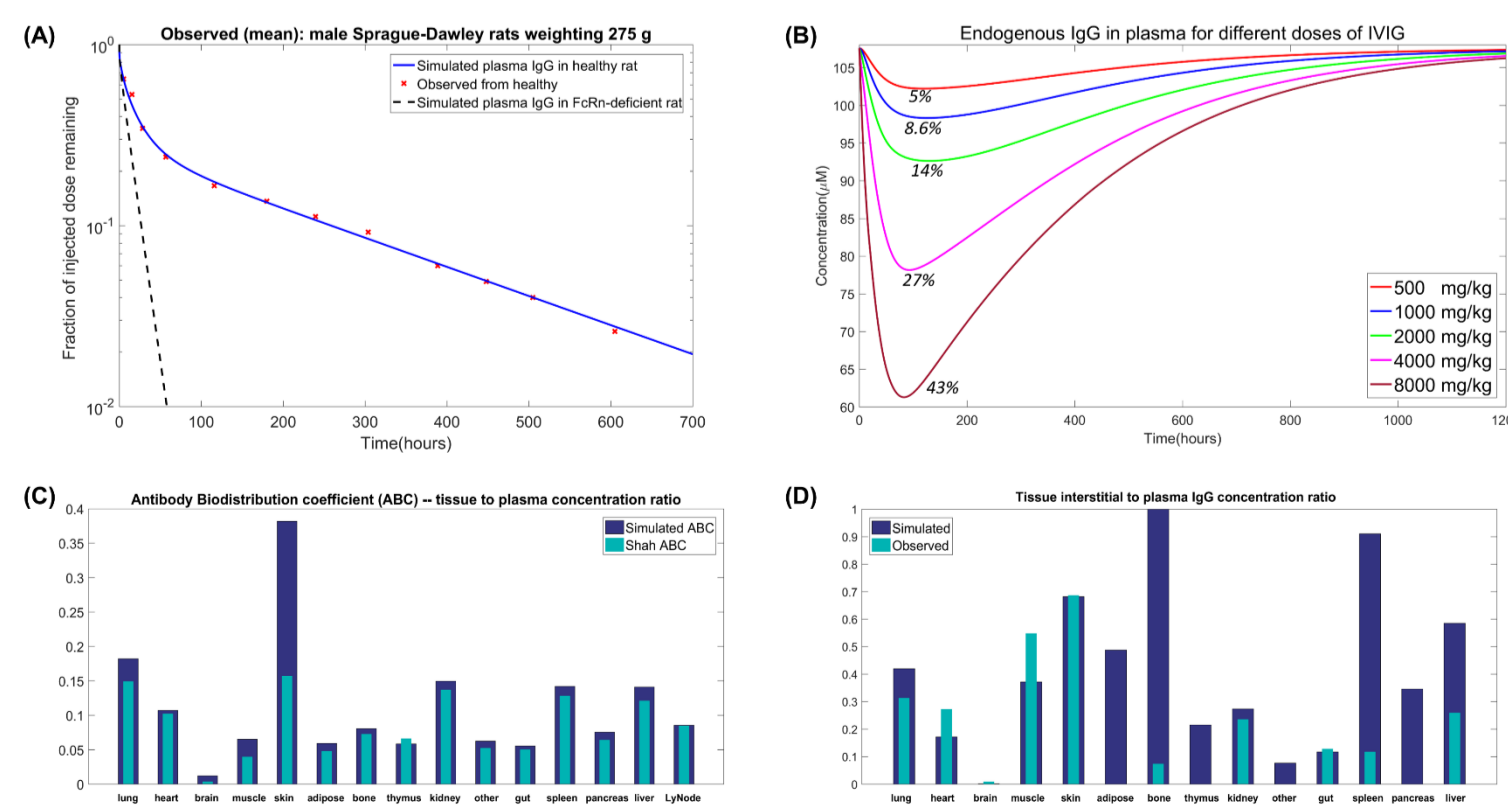


**Figure 2** (A) mean IgG profile and FcRn knockout effect. (B) IVIG. (C) Comparison of tissue to plasma IgG concentration ratios between the data generated from the current model and the data from Shah & Betts [9]. (D) Comparison of measured tissue interstitial IgG concentration to the model generated ones.

**Results (Con't): vc-MMAE ADC plasma profiles:** It was found that the base model can't match vc-MMAE profiles, and thus a plasma clearance was incorporated. Although a uniform plasma clearance for all ADC DAR species can match conjugated MMAE well, the total antibody profile has a very short half-life of 3.2 days. It is known that the total Ab profile for this ADC has a long half-life over 13 days, and thus a DAR-dependent plasma clearance becomes necessary. More details are given in Figure 4 (A), (B) & (C).

**Prediction of vc-MMAE ADC tissue profiles:** Simulated tissue uptakes of conjugated and unconjugated MMAE capture measured data in most of tissues, except lung, skin, muscle (not shown).

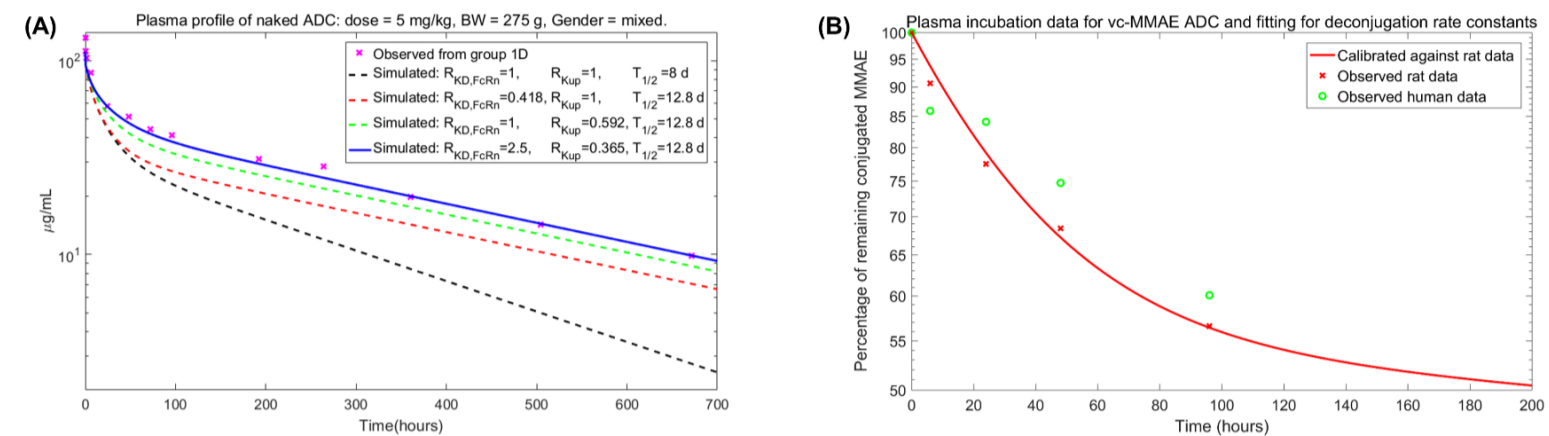


**Figure 3** (A) Matching the naked Ab plasma profile. From [6], binding affinity to rat FcRn at pH 6.0: human IgG1  $K_D = 35$  nM, rat IgG2a  $K_D = 14$  nM. Thus a factor  $R_{KD, FcRn} = 2.5$  is derived, which corrects the binding affinity of IgG to rFcRn in the model. Then reducing the fluid phase uptake rate by a factor  $R_{Kup} = 0.365$  enables the match of the naked Ab plasma profile. (B) *In vitro* metabolism of vc-MMAE ADC in rat and human plasma.

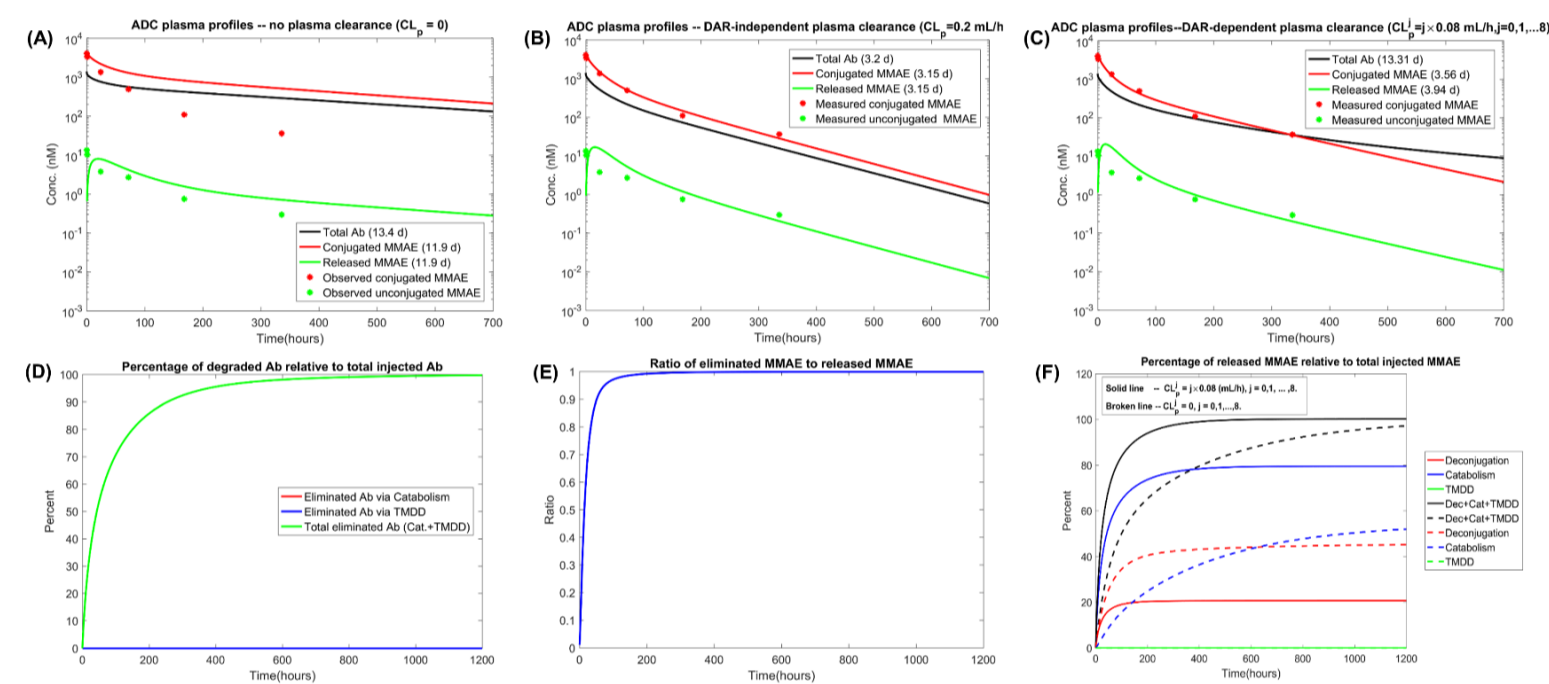


**Figure 4** The observed profiles are the mean profiles of 3 subjects. (A) Base model without plasma clearance can't match plasma profiles of vc-MMAE ADC. (B) A constant plasma clearance being uniformly applied to all DAR species can match the profiles, but the resulting total Ab profile has a very short half-life 3.2 days compared to an observed value over 13 days. (C) Using a calibrated DAR-dependent plasma clearance matches the profiles without shortening the half-life of total Ab. (D) Percentage of eliminated Ab relative to total injected Ab (accumulated). (E) Ratio of eliminated MMAE to released MMAE (accumulated). (F) Percentage of released MMAE relative to total injected MMAE (accumulated).

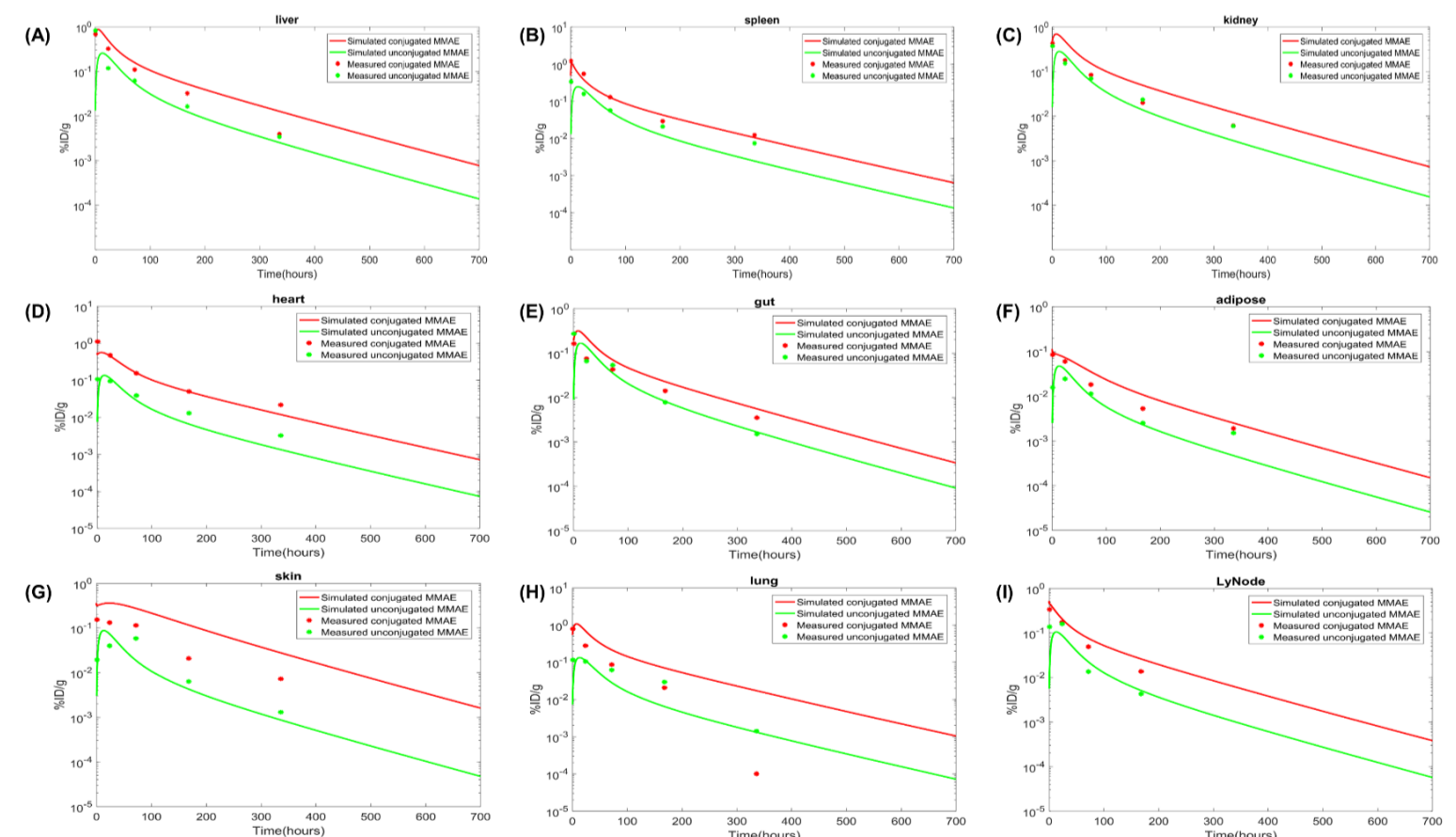


**Figure 5** Predicted and observed tissue profiles of conjugated MMAE and unconjugated MMAE in terms of percentage of injected dose per gram tissue (%ID/g). The observed profiles are the mean profiles of 3 subjects.

**Conclusion:** The developed full PBPK model can be used to simulate both mAbs and ADCs. The model is capable of capturing both IgG and mAb profiles. In the simulation study for a vc-MMAE ADC, it was found that a DAR-dependent plasma clearance is necessary to capture ADC profiles and deconjugation rates derived from *in vitro* measurement can be directly applied to simulations.

The developed full PBPK model for ADCs provides a useful platform to study the integrated effect of different processes on ADC disposition. The model was successful in predicting the *in vivo* ADC disposition in rat using available physiological and *in vitro* data together with a fundamental understanding of the mechanisms of ADC disposition.

## References:

- [1] Li L et al. *AAPS J.* (2014) 16(5): 1097-109.
- [2] Gibiansky L et al. *J PKPD.* (2014) 41(1): 35-47.
- [3] Fan Y et al. *mAbs* (2016) 8(5): 848-53.
- [4] Gill L et al. *AAPS J.* (2015) 18(1): 156-70.
- [5] Chen N et al. *mAbs* (2014) 6(2): 502-8.
- [6] Neuber T et al. *mAbs* (2014) 6(4): 928-42.
- [7] Bazin MJ et al. *J Pharm Pharmacol.* (1997) 49(3): 277-81.
- [8] Abdiche YN et al. *mAbs* (2015) 7(2): 331-343.
- [9] Shah DK et al. *mAbs* (2013) 5(2):297-305.